

Voxel Printing Anatomy: Design and Fabrication of Realistic, Presurgical Planning Models through Bitmap Printing

Nicholas M. Jacobson¹, Lawrence Smith², Jane Brusilovsky¹, Erik Carrera¹, Hayden McClain¹, Robert MacCurdy²

¹Inworks Innovation Initiative, University of Colorado-Anschutz ²Department of Mechanical Engineering, University of Colorado-Boulder

Corresponding Author

Nicholas M. Jacobson

Nicholas.Jacobson@Cuanschutz.edu

Citation

Jacobson, N.M., Smith, L., Brusilovsky, J., Carrera, E., McClain, H., MacCurdy, R. Voxel Printing Anatomy: Design and Fabrication of Realistic, Presurgical Planning Models through Bitmap Printing. *J. Vis. Exp.* (180), e63214, doi:10.3791/63214 (2022).

Date Published

February 9, 2022

DOI

10.3791/63214

URL

jove.com/video/63214

Abstract

Most applications of 3-dimensional (3D) printing for presurgical planning have been limited to bony structures and simple morphological descriptions of complex organs due to the fundamental limitations in accuracy, quality, and efficiency of the current modeling paradigm. This has largely ignored the soft tissue critical to most surgical specialties where the interior of an object matters and anatomical boundaries transition gradually. Therefore, the needs of the biomedical industry to replicate human tissue, which displays multiple scales of organization and varying material distributions, necessitate new forms of representation.

Presented here is a novel technique to create 3D models directly from medical images, which are superior in spatial and contrast resolution to current 3D modeling methods and contain previously unachievable spatial fidelity and soft tissue differentiation. Also presented are empirical measurements of novel, additively manufactured composites that span the gamut of material stiffnesses seen in soft biological tissues from MRI and CT. These unique volumetric design and printing methods allow for deterministic and continuous adjustment of material stiffness and color. This capability enables an entirely new application of additive manufacturing to presurgical planning: mechanical realism. As a natural complement to existing models that provide appearance matching, these new models also allow medical professionals to "feel" the spatially varying material properties of a tissue simulant—a critical addition to a field in which tactile sensation plays a key role.

Introduction

Currently, surgeons study numerous discrete 2-dimensional (2D) imaging modalities displaying distinct data to plan for operations on 3D patients. Furthermore, viewing this data on a 2D screen is not fully capable of communicating

the full extent of the collected data. As the number of imaging modalities grows, the ability to synthesize more data from distinct modalities, which exhibit multiple scales of organization, necessitates new forms of digital and physical representation to condense and curate information for more effective and efficient surgical planning.

3D-printed, patient-specific models have emerged as a new diagnostic tool for surgical planning that has been shown to reduce operating time and surgical complications¹. However, the process is time-consuming due to the standard stereolithography (STL) method of 3D printing, which shows a visible loss of data and renders printed objects as solid, homogeneous, and isotropic materials. As a result, 3D printing for surgical planning has been limited to bony structures and simple morphological descriptions of complex organs². This limitation is a result of an outdated manufacturing paradigm guided by the products and needs of the industrial revolution, where manufactured objects are fully described by their exterior boundaries³. However, the needs of the biomedical industry to replicate human tissue, which displays multiple scales of organization and varying material distributions, necessitate new forms of representation that represent the variations across the entire volume, which change point by point.

To address this issue, a 3D visualization and modeling technique (**Figure 1**) was developed and coupled with a novel, additive manufacturing process that enables greater control over the mixing and deposition of resins in ultrahigh resolution. This method, called bitmap printing, replicates human anatomy by 3D printing directly from medical images at a level of spatial fidelity and spatial/contrast resolution of advanced imaging technology approaching 15 μm . This enables the precise and graduated control required to

replicate variations in morphologically complex soft tissue with no loss or alteration of data from diagnostic source images.

Protocol

NOTE: 3D Slicer Medical Image Computing Software⁴ (see the **Table of Materials**) was used for the work completed in sections 1 through 3.

1. Data input

1. Open the medical image computing software, click the **File** button and **DICOM** from the dropdown menu, and wait for the **DICOM Browser** window to open.
 1. In the **DICOM Browser** window, select **Import**. Wait for the **Import DICOM Files from directory** popup window to appear.
 2. Navigate to the **DICOM file stack** and click the **Import** button.
 3. Ensure that the selected stack of DICOM files are loaded into the **DICOM Browser**. Ensure that the data has been correctly populated and matches the desired study in the following categories: Patient, Study, Series, and Instance.
 1. Click the **Advanced** check box to activate additional metadata. Select the desired **Series Number** and click the **Examine** button. Ensure the desired sequence is not displaying warnings. Click the check box next to the desired **DICOM Data** file | **Load**.
- NOTE:** Select the highest resolution images with the thinnest slice acquisition as this method is capable of printing at 15 μm and 27 μm slice thickness.

2. For volume rendering, once the sequence is loaded into the medical image computing software, navigate to **Modules** and select **Volume Rendering Module** from the dropdown menu.

1. In the **Volume Rendering** module, select the name of the sequence from the **Volume** dropdown menu to activate the image stack and translate the data into a voxelized volume. Ensure that the active module's name matches the desired sequence selected in step 1.1.3.1.
2. Click the **Eye Ball** icon next to the **Volume** dropdown to visualize the selected volume in 3D. Ensure that the 3D display window is open and a grayscale 3D representation is visible.
3. Next, click the arrow next to **Advanced** to open the **Advanced Tools**. Select the **Volume Property** tab to open a set of controls for modifying the color channel of the voxel model.
4. Navigate to the **Scalar Opacity Mapping** menu. Left-click in the field to create points where intensity values will be defined by opacity. Place points along this scale to visualize the anatomy of interest.
NOTE: The right-left location of the point is correlated to the range of the image's intensity values, and the up-down location refers to the opacity.
5. Navigate to the **Scalar Color Mapping** menu. Left-click in the field to create points and specify colors correlated to intensity values. Double-click in the field to open a **Select Color** window to modify color information.

2. Manipulations

NOTE: A masking step is required if the anatomy is sufficiently complex, to the point where surrounding tissues and extraneous data are present after modifications to the **Volume Properties**.

1. Navigate to **Modules** and select the **Segment Editor** from the dropdown menu. Ensure the **Segment Editor** toolbars appear.
 1. Navigate to the **Segmentation** dropdown and select **Create New Segmentation as**. Type a custom name for the segmentation from the **Rename Segmentation** popup window and click **OK**.
 2. Navigate to the **Master Volume** dropdown and select the active volume, which will have the same name as the **Volume Rendering**. Next, click the **Add** button directly below the dropdown. Ensure the segment container is created in the field below.
 3. Navigate to the **effects tool** panel below and select the **Scissors** tool. Navigate to the **Scissors** menu and select **Fill Inside**, **Free-form**, and **Unlimited**. Next, hover over the **3D Window**, right-click and hold while drawing around the area to be erased. Ensure a colored swath appears, showing what has been covered. Repeat this process until all areas to be deleted are covered.
NOTE: There are **Extensions**, such as **Segment Editor Extra Effects**, that can be downloaded into the medical image computing software, containing tools for creating this segmentation.
 4. Next, select the **Mask Volume** tool from the **Effects** menu. Check **Select Inside** to delete all image data covered by the segment. Next, modify the Fill Value

to be -1000, which is equal to air, or void, in the Hounsfield unit scale. Finally, hit apply and click the **Eye Ball** next to the **Output Volume** to show the new masked volume.

1. Navigate to **Modules** and select **Volume Rendering** from the dropdown menu. Click the **Eye Ball** next to the active volume to turn off the visualization.
2. Next, from the dropdown menu, select the newly created **masked volume**. Click the **Eye Ball** to activate the volume.
3. Finally, navigate to the **Inputs** menu and open the **Properties** dropdown menu. Select the **Volume Property** created in step 1.2.5. Ensure the volume in the **3D View** is masked and color-encoded.

3. Slicing

NOTE: This process bypasses the traditional 3D printing method by sending the slice files directly to the 3D printing instead of an STL mesh file. In the following steps, slices will be created from the volume rendering. The **Bitmap Generator** module is a custom-built extension. This can be downloaded from **Extensions Manager**.

1. Navigate to the **Modules**, select **Slicerfab** from the dropdown. Ensure the **Print Parameters** and **Output Parameters** menus are present.
 1. Under the **Printer Parameters** dropdown, ensure the **X resolution** is set to **600 DPI** and the **Y resolution** is set to **300 DPI**. Ensure the **Layer thickness** is set to **27 µm**.
 2. Next, open the **Output Parameters** menu and modify the scale of the final model as needed.

3. Finally, select a file location for the slices to be saved and click **Generate**.

NOTE: This step can take several minutes to complete.

4. Dithering

NOTE: Adobe Photoshop (see the **Table of Materials**) was used for the work completed in section 4.

1. Open the image editing software and click **File** and select **Open** from the dropdown menu. Navigate to the first image of the PNG file stack created in the previous step and click the **Open** button.
2. Navigate to **Window** and select **Actions** from the dropdown menu. In the **Actions** menu, click **New Action**, enter a custom name, and select **OK**. Ensure the action is being recorded by checking that the **Record** button is active and red.
 1. Once the image has loaded, navigate to **Image | Mode | Indexed Color**. In the **Index** window, select from the dropdown menu **Local Perceptual** and specify the number of colors to be **8**.
 2. In the **Forced** menu, select **Custom**. Click the first two squares, wait for the **Custom Color** window to pop up, and select a custom color pallet. Select **100% Magenta** and ensure **C**, **Y**, and **K** are set to **0**.
 1. Repeat this process and ensure there are two squares devoted to **100% C**, **Y**, and **K**.
 3. In the **Options** menu, for **Matte**, select **Custom** from the dropdown menu. For **Dither**, select **Diffusion**, and for **Amount**, select **100%**. Finally, click **OK**.

4. Navigate to the **Action** menu and click the **square** button to stop recording. Close the active window and click **No** in the **save changes** popup window.
3. Navigate to **File | Automate | Batch**. In the **Batch** popup window, navigate to the **Action** dropdown and select the action created in the previous step. Next, under the **Source** menu, click the **Choose** button and navigate to the folder of images exported in step 3.1.3. Under the **Destination** menu, click the **Choose** button, select a destination folder location for the new files, and click **OK**.
2. On the **Tools** page under **Material Mapping**, select the material from the dropdown menu to be mapped to the associated color, derived from the PNG files. Repeat this process for each color in the menu. Then, click **Finish | OK** on the popup window **Info Gcvf creation succeeded**.
3. On the host computer print software, click **File | Import File** from the dropdown menu. Navigate to the **Gcvf file** and click **Load**. On the main screen, select **Print**.

5. Voxel printing

NOTE: Stratasys GrabCAD⁵ was used for the work completed in section 5.

1. Open the print software, click **Apps** and **Launch Voxel Print Utility** from the dropdown menu.
 1. In the **Slice Files' Prefix** text box, enter the prefix of the PNG file stack. Next, click the **Select** button and navigate to the folder where the PNG files stack is located, and click **OK**.
 2. Under **Slice Range**, ensure the **First Slice** and **Number of Slices** match the number of files in the created folder.
 3. Under **Slicing Parameters**, ensure the **Sliced thickness (mm)** matches the settings specified in step 3.1.1.1 and **Slice width (pixels)** and **Slice height (pixels)** match the PNG files width and height.
 4. Under **Background Color**, ensure the background matches the background color, set not to print. Once completed, click the **Next** button.

Representative Results

A positive result, as shown in **Figure 2** and **Figure 3**, will be a direct translation of the volume rendering as defined in steps 1.2.5 or 2.1.1.4. The final model should visually match the volume rendering in size, shape, and color. Along this process, there are numerous steps where an error can occur, which will affect one or more of the properties listed above.

Issues related to the uniform scaling, as shown in **Figure 4**, of the printed models can be a result of the imaging, the computer hardware, and/or default software settings. Hospitals use a variety of techniques to produce and render images from a range of possible scanners. As this method works directly from the source images, which can expose metadata not typically utilized, it is important to be familiar with the nuances of the imaging workflow. Issues of scale can arise when 'transformation' is baked into the metadata, which can artificially adjust layer height and rotation.

Scale issues can also be a result of the computer monitor size. Some versions of Slicerfab have been set to slice the volume rendering and save the resulting PNG to the size of the active screen. In these versions of Slicerfab, images that are larger than the monitor will be cut off. Finally, various updates in Photoshop have resulted in scale issues when the

updates modify the defaults to the image import resolution. When the default is set to anything other than 600 DPI, the images will not maintain the same scale of images produced by the medical image computing software. They will result in distortions to the X-Y dimension while the z height of the model will remain correct.

Issues related to irregular shapes and unexpected geometries can result when working with opacity in the medical image computing software. The **volume properties** tab contains the ability to modify both color and opacity channels. When the opacity channel is set below 50%, the rendering algorithms produce visualizations that are difficult for the user to perceive, particularly surrounding complex structures. This can result in additional data being parsed in the process and can lead to unwanted data being 3D printed.

Issues related to color can result from software graphics and user errors in both image editing software and print software. The medical image computing software has numerous

choices for adjusting the volume rendering. Although the current version of Slicerfab has hard-coded rendering settings, modifications can still be made. Activating light and shade settings, as well as GPU rendering settings, can produce unexpected and irreproducible results. Finally, the dithering steps starting at step 4.1.2.3 can impact color based on the options for color synthesis, which is determined by the number and relative concentrations of the available base materials in the printer.

The 'local perceptual' dithering algorithm attempts to produce a visual approximation of the source color from the available colors defined in the 'color picker.' Modifying the number and color of the base materials will modify the resulting hue and color accuracy of the printed model. Furthermore, if clear is used as a base material, as shown in **Figure 5**, issues surrounding surface and subsurface light scattering through the printed model often result in unfaithful color translations from the digital rendering to the printed model⁶.

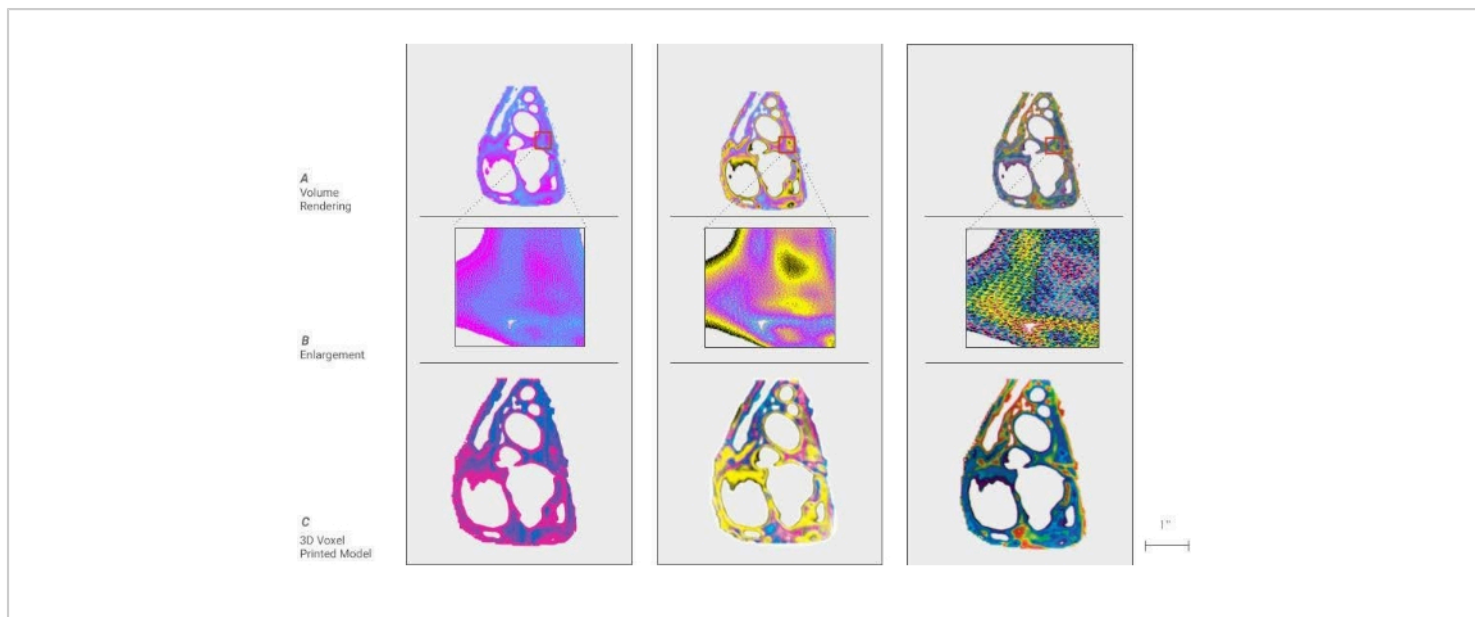


Figure 2: Voxel digital to physical dithering of color. (A) a cross-section of a cardiac model is shown by dividing the density ranges of the anatomy into 2, 4, and 10 colors. (B) An enlargement of a portion of each model is called out, showing the individual pixels, which will be processed to droplets of materials in the 3D printing process. (C) Shown here are cross-sectional 3D printed models using the voxel technique, demonstrating the translation from an image to the model. [Please click here to view a larger version of this figure.](#)

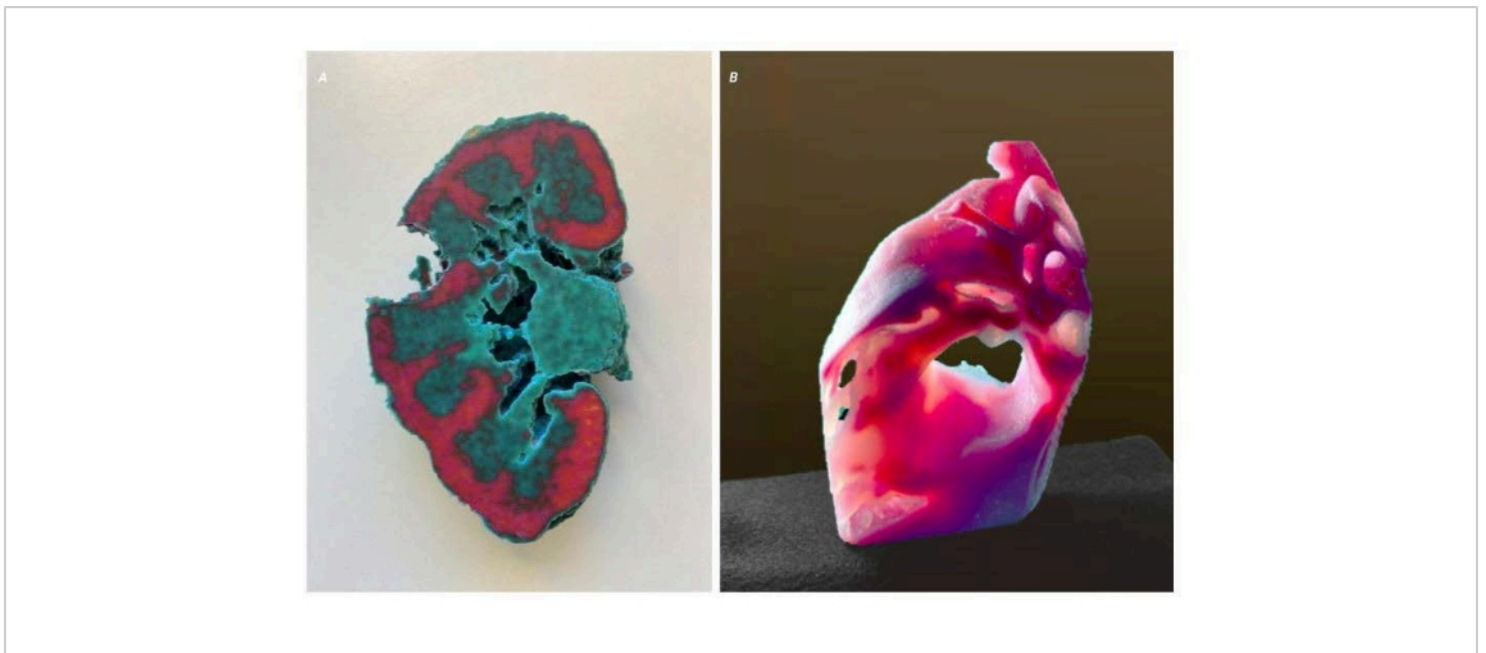


Figure 3: Voxel representative results. Two models displaying representative results of a successful method. **(A)** A cross-sectional kidney model of an adult with clear cell carcinoma. The tumor on the right side has been removed to show the interface between the kidney and tumor. This allows a surgeon a better understanding of the morphology of the tumor and its relationship to critical elements to be avoided. **(B)** A sectioned cardiac model showing the variation in tissue density. [Please click here to view a larger version of this figure.](#)

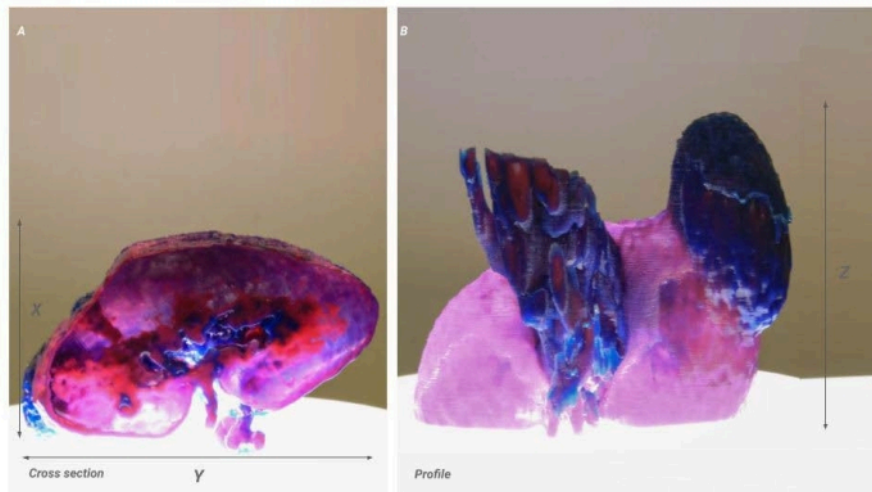


Figure 4: Voxel scale issue. Two images of the same model showing the result of a scaling issue. **(A)** Cross-sectional image of the kidney. The X-Y resolution is shown proportionally but is 50% of the intended product **(B)** Profile view of the kidney. The X-resolution remains accurate from the source data and results in a model that appears stretched in the X-direction. [Please click here to view a larger version of this figure.](#)



Figure 5: Potential problems. Two images of two different models demonstrate the issues around the clarity of working with translucent materials. **(A)** This model shows the result of enclosed voids within the model that have been filled with a 'support' material by the printer. In this model, the voids were intentionally created to create a variation in optical properties. **(B)** This model shows open voids that run deep into the model. The voids are tortuous, making standard postprocessing techniques, which polish the surface, impossible. The resulting optical distortion has rendered the model unusable for clinical applications. [Please click here to view a larger version of this figure.](#)

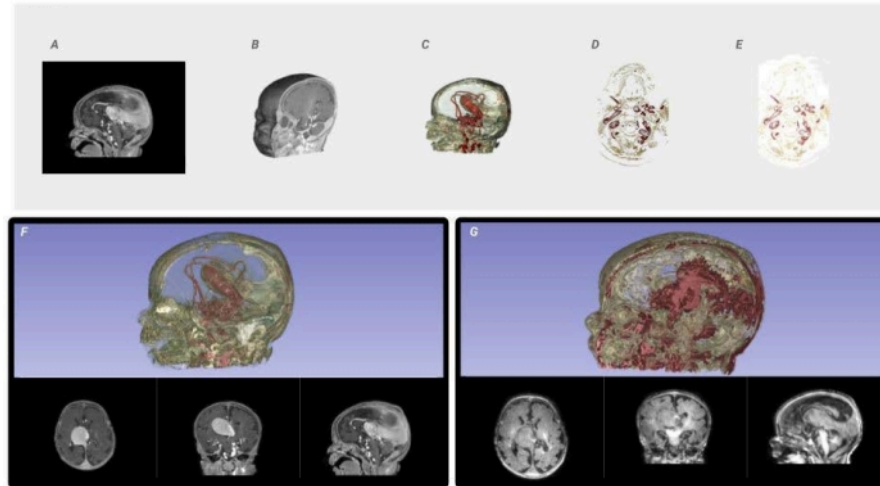


Figure 6: Voxel processing workflow and image quality comparison. From the input DICOM data, (A) a mask is created to isolate the area of interest and reconstruct it into a 3D Volume Rendering, (B) from which a histogram is analyzed to parse the ranges of intensity values. The shape channel of the voxel-based volume rendering is activated to visualize the form of the resulting masked DICOM. The material channel of the voxel-based volume rendering is modified, through lookup tables, which map color to the specified intensity ranges (C). The volume rendering is sliced as full-color PNG files to the required constraints and resolution of the printer (D). Every PNG slice is dithered into the material descriptions needed to fabricate the medical data. (E) The resulting color-composite PNGs are sent to the printer. (F) A visualization of a high-resolution data set compared to a low-resolution data set (G) using the same technique to demonstrate the need for the highest quality source data. [Please click here to view a larger version of this figure.](#)

Discussion

The current representational framework that the majority, if not all, of digital modeling tools employ today results in the STL file format⁸. Nevertheless, the specific nature of this paradigm has proven inadequate when trying to express the granular or hierarchical structure of more complex, natural materials. With the arrival of recent additive manufacturing techniques such as multimaterial 3D printing, highly tuned and highly optimized objects can be produced, which display gradual material transitions throughout their volume. This paper suggests that a voxel or bitmap-based process is

more suited to complex material representations and provides a technique for translating radiodensity and morphologic complexity from radiological images. The advantages of this workflow include i) a precise, graduated control over the material distribution at multiple scales within a 3D printed volume and ii) the power to increase existing 2D image processing techniques on 3D voxel fields and produce new creative avenues within the design and engineering of objects whose aesthetic qualities and material organization are highly modulated to suit their structural performance.

Every step in this process is critical to achieving an accurate final 3D print, and there is little room for error. Along the way, there are numerous points where extra attention is required, and checks should be performed to ensure accuracy. First, selecting the right images for this method has a direct impact on the final 3D printed model, as shown in **Figure 6F,G**. This method seeks to maintain the purity of the source images; any modifications to improve resolution or smooth contours could introduce or eliminate data. The final product in this method is only as good as the input data. This method allows for droplet resolution of 15 μm and 27 μm layer thickness. Therefore, it is critical to work closely with a radiologist to source the highest resolution images with the thinnest slice count.

Second, the model editing steps described in the protocol steps 1.1, 2, and **Figure 6A** require user input to mask and modify the lookup tables to extract and render the desired outcome. Due to the high level of resolution, multiple scales of an anatomical structure are editable. A thorough understanding of medical image data structures and their relation to biological tissues is critical to extracting the desired data. Attention during this step can allow for highly tuned models that replicate multiple scales of organization in biological tissue.

Third, the dithering step described in protocol step 4 determines how materials will be graduated from the source colors. It is critical to ensure the source colors relate to the colors in the printer. If the colors in the printer do not match the colors in the dithering step, unexpected variations in color can occur in the final model. Additionally, numerous dithering techniques will produce a variety of results. It is critical that this be examined closely to ensure that no data is lost, and the appropriate information is being displayed coherently.

We provide some troubleshooting solutions to the issues defined in the representative results. First, issues related to scale are generally related to a Transformation baked into the medical image metadata received from a radiological department. This issue can be corrected in the medical image computing software by deleting all these inherited 'Transformations.' The first step is to open the **Transformation** menu and select **Delete Active Transform** from the dropdown menu. Repeat this process for all inherited transformations; this should immediately correct the issue.

Second, issues related to geometry are generally related to activating the opacity channel in protocol step 1.2.4. When the opacity channel is set below 50%, the rendering algorithms produce visualizations, which are difficult for the user to perceive, particularly surrounding complex structures. The solution to this issue is to set the opacity channel to 100%, thus creating a solid color that can be defined as a 'clear' material in protocol step 5.

Third, issues related to slicing in the Slicerfab program are often a result of multiple 'Volumes' and the region of interest tool (**ROI**) being loaded in the medical image computing software. If multiple 'Volumes' are loaded, select the extraneous volumes from the **Volume** dropdown menu in the **Volume Rendering** module so that it is active. Next, from the same dropdown menu, select **Delete current Volume**. Repeat this step for an additional ROI that may have been created. When one 'Volume' and one 'ROI' are present, Slicerfab should work without the need for a restart.

Generally, all limitations of this protocol are related to hardware and related material availability. The current 3D printers used in this method are limited to 15 μm X-Y and 25 μm Z height resolution. This limitation is relevant when working with ultrahigh-resolution imaging data, such as Micro

CT, where image resolution can approach 5 mm and would cause this method to introduce error⁷. This printer is also limited to printing 7 base materials at any one time, which can limit the range of available colors.

Blending at the droplet level does occur, allowing for the potential of 25,000,000 possible color combinations that can be created by co-deposition. However, the exact mechanism of material blending at the droplet level prior to UV curing is not well known. Furthermore, the printed material requires significant postprocessing, leading to visual artifacts with interior voids and hard-to-reach features. Therefore, it is critical to evaluate the geometry prior to fabrication to ensure the desired visual clarity when interior voids and complex geometry will not allow for postprocessing.

Three-dimensional printing is currently used to fabricate models for surgical planning, implantation, and operative navigation, improving patient care during surgical procedures and across the hospital environment^{9,10}. However, the current adoption of 3D printed models for presurgical planning has been slow, partly due to the limited range of applications available with the current STL method for 3D printing. This method produces a loss in data and visible inaccuracies compared to the source data set, severely limited levels of complexity in relation to true anatomical morphology, and volumetric gradients of the original data that cannot be reproduced.

Although 3D printing morphologic data alone have proven to be successful, the range of applications with this method is limited to bony applications and simple geometric representations of complex anatomical features. In this process, valuable volumetric data are lost, which compromises the consistency and integrity of source data. Inversely, this method to extract the material composition of

the 3D-printed model without deviation from medical images avoids these issues. This method can reproduce medical images with greater accuracy with known advantages for surgical procedures where morphological accuracy is critical. The protocol in this paper describes the tactile visualization of medical data through submillimeter resolution, multimaterial, 3D voxel printing. The incorporation of soft resins, with durometers in the range analogous to human tissue, could foreseeably allow for the recreation of radiologically scanned soft tissue to be used with tactile planning methods during surgical preparation.

Disclosures

N.J. is an author on a patent application filed by the University of Colorado Regents that describes methods like those described in this work (application no. US16/375,132; publication no. US20200316868A1; filed 04 April 2019; published 08 October 2020). All other authors declare that they have no competing interests.

Acknowledgments

We thank AB Nexus and the State of Colorado for their generous support of our scientific research into voxel printing for presurgical planning. We thank L. Browne, N. Stence, and S. Sheridan for providing data sets used in this study. This study was funded by the AB Nexus Grant and the State of Colorado Advanced Industries Grant.

References

1. Ali, A. et al. Clinical situations for which 3D printing is considered an appropriate representation or extension of data contained in a medical imaging examination: adult cardiac conditions. *3D Printing in Medicine*. **6** (1), 24 (2020).

2. Ballard, D. H. et al. Radiological Society of North America (RSNA) 3D Printing Special Interest Group (SIG) clinical situations for which 3D printing is considered an appropriate representation or extension of data contained in a medical imaging examination: abdominal, hepatobiliary, and gastrointestinal conditions. *3D Printing in Medicine*. **6** (1), 13 (2020).
3. Corney, J. The next and last industrial revolution? *Assembly Automation*. **25** (4) (2005).
4. 3D Slicer image computing platform. <https://www.slicer.org/>. Fedorov A. et al. 3D Slicer as an image computing platform for the quantitative imaging network. *Magnetic Resonance Imaging*. **30** (9), 1323-1341 (2012).
5. *GrabCAD Guide to Voxel Printing*. <https://help.grabcad.com/article/230-guide-to-voxel-printing?locale=en>. (2022).
6. Bader, C. et al. Making data matter: Voxel printing for the digital fabrication of data across scales and domains. *Science Advances*. **4** (5), eaas8652 (2018).
7. Zhang, F., Li, C., Wang, Z., Zhang, J., Wang, Y. Multimaterial 3D printing for arbitrary distribution with nanoscale resolution. *Nanomaterials*. **9** (8), 1108 (2019).
8. Robson, R. The STL Algorithms. In *Using the STL*. Springer, New York, NY, 47-54 (1998).
9. Waran, V., Narayanan, V., Karuppiah, R., Owen, S. L. F., Aziz, T. Utility of multimaterial 3D printers in creating models with pathological entities to enhance the training experience of neurosurgeons. *Journal of Neurosurgery*. **120** (2), 489-492 (2014).
10. Cumbler, E. et al. Contingency planning for healthcare worker masks in case of medical supply chain failure: Lessons learned in novel mask manufacturing from COVID-19 pandemic. *American Journal of Infection Control*. **49** (10), 1215-1220 (2021).